Investigation of the Electronic and Geometric Effects of Trifluoromethyl Substituents on Tris(pyrazolyl)borate Ligands Using Manganese(I) and Copper(I) Complexes

H. V. Rasika Dias,* Hyoung-Juhn Kim, Hui-Ling Lu, Krishnan Rajeshwar,*
Norma R. de Tacconi, Agnes Derecskei-Kovacs, and Dennis S. Marynick*

Department of Chemistry and Biochemistry, The University of Texas at Arlington,
Arlington, Texas 76019-0065

Received February 1, 1996[⊗]

Manganese tricarbonyl complexes of fluorinated tris(pyrazolyl)borate ligands $[HB(3,5\text{-}(CF_3)_2Pz)_3]^-$ and $[HB(3\text{-}(CF_3)Pz)_3]^-$ (where Pz = pyrazolyl) were synthesized by treating $BrMn(CO)_5$ with $[HB(3,5\text{-}(CF_3)_2Pz)_3]Ag(THF)$ or $[HB(3\text{-}(CF_3)Pz)_3]Na(THF)$. The reaction of $[HB(3\text{-}(CF_3)Pz)_3]Na(THF)$ with copper(I) trifluoromethanesulfonate under CO afforded $[HB(3\text{-}(CF_3)Pz)_3]CuCO$. Compounds $[HB(3,5\text{-}(CF_3)_2Pz)_3]Mn(CO)_3$ (**5**), $[HB(3\text{-}(CF_3)Pz)_3]Mn(CO)_3$ (**6**), and $[HB(3\text{-}(CF_3)Pz)_3]CuCO$ (**7**) were characterized by ^1H NMR, ^{19}F NMR, and IR spectroscopy and by X-ray crystallography. They have relatively high C−O stretching frequencies. However, the ν_{CO} values are much lower than that in free CO and the relative lowering is higher for manganese adducts. The CF_3 substitution on the 5-position has a significant effect on the metal center. This is readily apparent from the infrared spectroscopic data. Theoretical calculations of the geometries of [tris(pyrazolyl)borato]manganese(I) and -copper(I) carbonyls are in excellent agreement with the experimental results. Increasing the degree of fluorination lengthens the metal−C and metal−N bonds and shortens the C−O distance. The metal−Pz bonding is essentially a pure σ-interaction. Cyclic voltammetry data for the copper complexes show high oxidation potentials for the fluorinated analogs. IR spectroscopic data of the [tris(pyrazolyl)borato]manganese and -copper carbonyls have also been compared to those of cyclopentadienyl analogs.

Introduction

Poly(pyrazolyl)borates have been used extensively in inorganic, organometallic, and bioinorganic chemistry.[1−4] Among the many varieties of poly(pyrazolyl)borates, the tris(pyrazolyl)borate ligand has attracted the most interest, perhaps due to its close analogy to the ubiquitous cyclopentadienyl system.[1] In fact, complexes of tris(pyrazolyl)borate ligands are now known for most of the metals in the periodic table. Interestingly, the vast majority of studies involving the metal complexes of tris(pyrazolyl)borates are limited to the parent ligand $[HB(Pz)_3]^-$ (**1**) or their alkyl-substituted derivatives such as $[HB(3,5\text{-}(CH_3)_2Pz)_3]^-$ (**2**) and $[HB(3,5\text{-}(i\text{-}Pr)_2Pz)_3]^-$ (or to a lesser extent the aryl-substituted ligands). Considering the unique properties of fluorinated ligands[5−7] and their importance in a variety of applications,[6,8−17] it is surprising that very little is known about the tris(pyrazolyl)borates bearing fluoroalkyl substituents.[1]

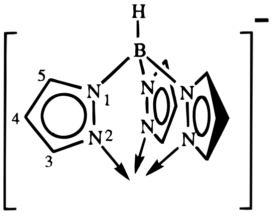

1

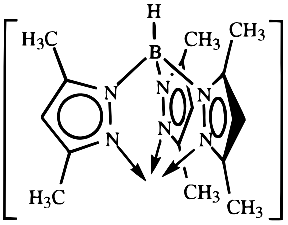

2

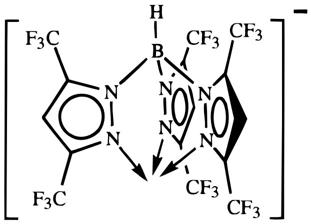

3

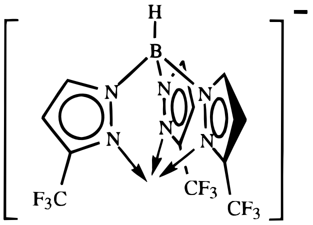

4

One area of our research focus is the development of fluorinated poly(pyrazolyl)borate ligands and the chem-

---

* To whom correspondence should be addressed.

[⊗] Abstract published in *Advance ACS Abstracts,* June 1, 1996.

(1) Trofimenko, S. *Chem. Rev.* **1993**, *93*, 943.

(2) Trofimenko, S. *Prog. Inorg. Chem.* **1986**, *34*, 115.

(3) Shaver, A. In *Comprehensive Coordination Chemistry*; Wilkinson, G., Gillard, R. D., McCleverty, J. A., Eds.; Pergamon: New York, 1987; Vol. 2, p 245.

(4) Niedenzu, K.; Trofimenko, S. *Top. Curr. Chem.* **1986**, *131*, 1.

(5) Witt, M.; Roesky, H. W. *Prog. Inorg. Chem.* **1992**, *40*, 353.

(6) *Inorganic Fluorine Chemistry, Toward the 21st Century;* ACS Symposium Series 555; Thrasher, J. S., Strauss, S. H., Eds.; American Chemical Society: Washington, DC, 1994.

(7) Morrison, J. A. *Adv. Organomet. Chem.* **1993**, *35*, 211.

(8) Horvath, I. T.; Rabai, J. *Science* **1994**, *266*, 72.

(9) Gladysz, J. A. *Science* **1994**, *266*, 55.

(10) Burk, M. J.; Feng, S.; Gross, M. F.; Tumas, W. *J. Am. Chem. Soc.* **1995**, *117*, 8277.

(11) Bonnemann, H. *Angew. Chem., Int. Ed. Engl.* **1985**, *24*, 248.

(12) Bonnemann, H.; Brijoux, W.; Brinkmann, R.; Meurers, W.; Mynott, R. *J. Organomet. Chem.* **1984**, *272*, 231.

(13) Kiplinger, J. L.; Richmond, T. G.; Osterberg, C. E. *Chem. Rev.* **1994**, *94*, 373.

(14) Schrock, R. R. *Acc. Chem. Res.* **1990**, *23*, 158.

(15) Hampden-Smith, M. J.; Kodas, T. T. *Polyhedron* **1995**, *14*, 699.

(16) Strauss, S. H. *Chem. Rev.* **1993**, *93*, 927.

(17) Aubke, F.; Wang, C. *Coord. Chem. Rev.* **1994**, *137*, 483.

S0276-7333(96)00065-9 CCC: $12.00

istry of their metal complexes.[18−24] We are particularly interested in investigating the effects of fluoro substituents on the physical properties and chemical reactivity of the metal adducts. Recently, we reported the synthesis of two highly fluorinated ligand systems, $[HB(3,5\text{-}(CF_3)_2Pz)_3]^-$ (**3**) and $[HB(3\text{-}(CF_3)Pz)_3]^-$ (**4**).[18,19] These ligands have been found to be very useful in stabilizing novel species such as $[HB(3,5\text{-}(CF_3)_2Pz)_3]AgCO$, $[HB(3,5\text{-}(CF_3)_2Pz)_3]AuCO$, and $[HB(3,5\text{-}(CF_3)_2Pz)_3]In$.[21,22,25]

This paper concerns the results from our investigation of the electronic and geometrical effects of fluorinated tris(pyrazolyl)borate ligands. We report the syntheses and X-ray crystal structures of the manganese carbonyl complexes $[HB(3,5\text{-}(CF_3)_2Pz)_3]Mn(CO)_3$ (**5**) and $[HB(3\text{-}(CF_3)Pz)_3]Mn(CO)_3$ (**6**) and the copper carbonyl complex $[HB(3\text{-}(CF_3)Pz)_3]CuCO$ (**7**) and contrast their spectroscopic and structural data with those of the nonfluorinated analogs. In order to better understand the electronic effects of CF_3 substituents on the tris(pyrazolyl)borate ligands, we have also carried out a molecular orbital study of the Mn(I) and Cu(I) carbonyl systems. Cyclic voltammetry data for the fluorinated and non-fluorinated [tris(pyrazolyl)borato]copper complexes are also presented.

Experimental Section

General Procedures. All manipulations were carried out under an atmosphere of purified nitrogen using either standard Schlenk techniques or a Vacuum Atmospheres single-station drybox equipped with a −25 °C refrigerator. Solvents were purchased from commercial sources, distilled from conventional drying agents, and degassed twice prior to use.[26] Glassware was oven-dried at 150 °C overnight. The NMR spectra were recorded at 25 °C on a Bruker MSL-300 spectrometer (^1H, 300.15 MHz; ^{19}F, 282.36 MHz). Chemical shifts for ^1H NMR spectra are relative to internal Me_4Si or to residual protium in the deuterated solvents (C_6D_6, 7.15 ppm). ^{19}F NMR chemical shifts were referenced relative to external $CFCl_3$. IR spectra were recorded on a Bio-Rad 40S spectrometer. Melting points were obtained on a Mel-Temp II apparatus and were not corrected. Elemental analyses were performed using a Perkin-Elmer Model 2400 instrument. $Mn(CO)_5Br$ (Strem), di(copper(I) bis(trifluoromethanesulfonate)−benzene (Alfa), and CO (Matheson) were purchased and used as received. Syntheses of $[HB(3,5\text{-}(CF_3)_2Pz)_3]Ag(THF)$, $[HB(3\text{-}(CF_3)Pz)_3]Na(THF)$, and $[HB(3,5\text{-}(CF_3)_2Pz)_3]Na(THF)$ were carried out as reported previously.[19,22] $Cu(CH_3CN)_4BF_4$ was prepared by following a procedure analogous to that reported for the synthesis of its PF_6^- salt[27] but using aqueous HBF_4 instead of HPF_6.

Preparation of $[HB(3,5\text{-}(CF_3)_2Pz)_3]Mn(CO)_3$ (5). $[HB(3,5\text{-}(CF_3)_2Pz)_3]Ag(THF)$ (1.0 g, 1.25 mmol) in THF (20 mL) was added to $BrMn(CO)_5$ (0.41 g, 1.5 mmol) in THF (20 mL) at room temperature. The reaction mixture was stirred for 12 h. A greenish black precipitate was observed. The volatiles were removed under vacuum, and the residue was extracted into hexane. This extract was filtered, and the filtrate was concentrated to obtain yellow crystals (0.75 g, 79% yield). X-ray-quality crystals were grown from *n*-hexane at −20 °C. Mp: dec at 173 °C. ^1H NMR (C_6D_6): δ 6.22 (s, C*H*). ^{19}F NMR (C_6D_6): δ −57.2 (s), −58.7 (d, $^5J(H,F)$ = 2.1 Hz). IR (KBr; cm^{-1}): 2642 (B−H), 2065, 1975 (CO). Anal. Calcd for $C_{18}H_4BF_{18}MnN_6O_3$: C, 28.45; H, 0.53; N, 11.06. Found C, 28.92; H, 0.24; N, 10.87.

Preparation of $[HB(3\text{-}(CF_3)Pz)_3]Mn(CO)_3$ (6). $BrMn(CO)_5$ (0.43 g, 0.83 mmol) was dissolved in THF (20 mL) and treated with $[HB(3\text{-}(CF_3)Pz)_3]Na(THF)$ (0.23 g, 0.83 mmol) in THF at room temperature. The mixture was stirred for 24 h. The resulting mixture was filtered over Celite, and the volatiles were removed under reduced pressure. The residue was washed with *n*-hexane, extracted into toluene, and filtered. The solvent was removed under vacuum to obtain a yellow solid (0.3 g, 65% yield). X-ray-quality crystals were grown from methylene chloride at −20 °C. Mp: dec at 179 °C. ^1H NMR (C_6D_6): δ 6.90 (d, 3H, *J* = 1.5 Hz, C*H*), 6.01 (d, 3H, *J* = 1.5 Hz, C*H*). ^{19}F NMR (C_6D_6): δ −57.4 (s). IR (KBr; cm^{-1}): 2505 (B−H), 2054, 1963 (CO) cm^{-1}. Anal. Calcd for $C_{15}H_7BF_9MnN_6O_3$: C, 32.40; H, 1.27; N, 15.12. Found: C, 32.51; H, 0.93; N, 15.30.

Preparation of $[HB(3\text{-}(CF_3)Pz)_3]CuCO$ (7). $[HB(3\text{-}(CF_3)Pz)_3]Na(THF)$ (0.35 g, 0.68 mmol) in THF (10 mL) was added to a CO-saturated THF (20 mL) solution of di(copper(I) bis(trifluoromethanesulfonate)−benzene (0.17 g, 0.34 mmol) at room temperature. The mixture was stirred for 12 h under a CO atmosphere. The solvent was removed under vacuum, and the residue was extracted into methylene chloride. The resulting mixture was filtered over Celite, and the filtrate was concentrated and cooled to 0 °C to obtain **7** as a colorless solid (0.25 g, yield 72%). X-ray-quality crystals were obtained at −20 °C from a THF−toluene solution. Mp: 192−193 °C. ^1H NMR ($CDCl_3$): δ 6.50 (d, *J* = 1.7 Hz, 3H, C*H*), 7.67 (d, *J* = 1.7 Hz, 3H, C*H*). ^{19}F NMR ($CDCl_3$): δ −61.8 (s). IR (KBr; cm^{-1}): 2507 (B−H), 2100 (CO). Anal. Calcd for $C_{13}H_7BCuF_9N_6O$: C, 30.70; H, 1.39; N, 16.52. Found: C, 30.60; H, 1.43; N, 16.27.

Preparation of $[HB(3,5\text{-}(CF_3)_2Pz)_3]CuNCCH_3$. $Cu(CH_3CN)_4BF_4$ (0.157 mg, 0.499 mmol) and $[HB(3,5\text{-}(CF_3)_2Pz)_3]Na(THF)$ (0.500 mg, 0.698 mmol) were mixed in CH_2Cl_2 and stirred overnight at room temperature. During this period a white precipitate was formed. The mixture was filtered, and the volatile materials were removed under reduced pressure. The residue was washed with *n*-hexane and dried under vacuum to obtain $[HB(3,5\text{-}(CF_3)_2Pz)_3]CuNCCH_3$ in 91% yield. ^1H NMR (C_6D_6): δ 0.65 (s, 3H, CH_3), 6.26 (s, 3H, C*H*). ^{19}F NMR (C_6D_6): δ −58.5 (d, ^5J (H,F) = 3.3 Hz), −61.6 (s). Anal. Calcd for $C_{17}H_7N_7F_{18}BCu$: C, 28.14; H, 0.97; N, 13.51. Found: C, 28.59; H, 1.04; N, 13.74.

Crystallographic Data Collection and Structure Determinations. $[HB(3,5\text{-}(CF_3)_2Pz)_3]Mn(CO)_3$ (5). A suitable crystal of **5** with dimensions 0.30 × 0.31 × 0.60 mm was mounted on a glass fiber with a small amount of Paratone-N oil/grease and placed in the dinitrogen cold stream of a Siemens P4 diffractometer equipped with a LT-2A device.[28] Cell parameters were determined using 22 reflections. Data were corrected for Lorentz/polarization and for absorption effects. The space group determination was based upon a check of Laue symmetry and symmetric absences present and was confirmed by the structure solution. The structure was solved by direct methods followed by successive cycles of full-matrix least-squares refinement and difference Fourier analysis using the Siemens SHELXTL (PC version 5) software package.[29] The molecule crystallizes in the $P2_1/c$ space group. A rotational disorder (over two sites) was observed for the CF_3 group on C13. This disorder was modeled successfully, and the occupancies were refined to 48% and 52%. All non-

---

(18) Dias, H. V. R.; Lu, H.-L.; Ratcliff, R. E.; Bott, S. G. *Inorg. Chem.* **1995**, *34*, 1975.

(19) Dias, H. V. R.; Jin, W.; Kim, H.-J.; Lu, H.-L. *Inorg. Chem.* **1996**, *35*, 2317.

(20) Dias, H. V. R.; Lu, H.-L. *Inorg. Chem.* **1995**, *34*, 5380.

(21) Dias, H. V. R.; Jin, W. *J. Am. Chem. Soc.* **1995**, *117*, 11381.

(22) Dias, H. V. R.; Jin, W. *Inorg. Chem.* **1996**, *35*, 267.

(23) Dias, H. V. R.; Gorden, J. D. *Inorg. Chem.* **1996**, *35*, 318.

(24) Dias, H. V. R.; Lu, H.-L.; Gorden, J. D.; Jin, W. *Inorg. Chem.* **1996**, *35*, 2149.

(25) Dias, H. V. R.; Jin, W. *Inorg. Chem.*, in press.

(26) Perrin, D. D.; Armarego, W. L. F.; Perrin, D. R. *Purification of Laboratory Chemicals*; Pergamon: New York, 1985.

(27) Kubas, G. J. *Inorg. Synth.* **1979**, *19*, 90.

(28) Hope, H. In *Experimental Organometallic Chemistry;* ACS Symposium Series 357; Wayda, A. L., Darensbourg, M. Y., Eds.; American Chemical Society: Washington, DC, 1987; p 257.

(29) Siemens SHELXTL (PC version 5.0); Siemens Industrial Automation, Inc., Madison, WI.

Table 1. Crystal Data and Summary of Data Collection and Refinement

	$[HB(3,5-(CF_3)_2Pz)_3]Mn(CO)_3$	$[HB(3-(CF_3)Pz)_3]Mn(CO)_3$	$[HB(3-(CF_3)Pz)_3]CuCO$
formula	$C_{18}H_4BF_{18}MnN_6O_3$	$C_{15}H_7BF_9MnN_6O_3$	$C_{13}H_7BCuF_9N_6O$
fw	760.02	556.02	508.60
cryst size, mm	0.60 × 0.31 × 0.30	0.59 × 0.29 × 0.21	0.48 × 0.37 ×0.17
cryst syst	monoclinic	monoclinic	orthorhombic
space group	$P2_1/c$	$C2/c$	$Pnma$
a, Å	14.804(5)	25.366(2)	16.193(2)
b, Å	15.165(3)	8.9897(12)	13.486(2)
c, Å	12.092(4)	20.877(2)	8.2757(7)
α, deg	90	90	90
β, deg	113.90(2)	123.696(4)	90
γ, deg	90	90	90
V, Å^3	2481.8(12)	3960.7(7)	1807.3(4)
Z	4	8	4
D_{calc}, g/cm^3	2.034	1.865	1.869
μ(Mo Ka, 0.710 73 Å), mm^{-1}	0.706	0.784	1.318
F(000)	1480	2192	1000
T, K	183	183	183
2θ max, deg	47	45	50
R, wR2 ($I > 2\sigma(I)$)[a]	0.0415, 0.0995	0.0435, 0.0902	0.0350, 0.0861
R, wR2 (all data)	0.0560, 0.1091	0.0699, 0.1020	0.0457, 0.0923
no. of data, parms	3671, 452	2598, 319	1662, 159
largest diff peak and hole, e Å^{-3}	0.525, −0.503	0.518, −0.390	0.647, −0.504

[a] $R = \sum(||F_o| - |F_c||)/\sum|F_o|$; $wR2 = [\sum[w(F_o^2 - F_c^2)^2]/\sum[w(F_o^2)^2]]^{1/2}$.

hydrogen atoms were refined anisotropically. The hydrogen on B was located from the difference map and refined with a fixed U(H) value. The pyrazole ring hydrogens were included in the model at calculated positions ($U(H) = 1.2[U(C)]$).

$[HB(3-(CF_3)Pz)_3]Mn(CO)_3$ (6). A suitable crystal of **6** with dimensions 0.21 × 0.29 × 0.59 mm was used for the data collection. Cell parameters were determined using 40 reflections. Data were corrected for Lorentz/polarization and for absorption effects. The space group determination was based upon a check of Laue symmetry and symmetric absences present and was confirmed by the structure solution. Compound **6** crystallized in the $C2/c$ space group. The structure was solved by Patterson methods followed by successive cycles of full-matrix least-squares refinement and difference Fourier analysis using the Siemens SHELXTL (PC version 5) software package.[29] All the non-hydrogen atoms were refined anisotropically. The hydrogen on B was located from the difference map and refined with a fixed U(H) value. The remaining hydrogens were included in calculated positions ($U(H) = 1.2[U(C)]$).

$[HB(3-(CF_3)Pz)_3]CuCO$ (7). A suitable crystal of **7** with dimensions 0.17 × 0.37 × 0.48 mm was used for the data collection. Cell parameters were determined using 47 reflections. Data were corrected for Lorentz/polarization and for absorption effects. The space group determination was based upon a check of Laue symmetry and symmetric absences present and was confirmed by the structure solution. Compound **7** crystallized in the $Pnma$ space group with a crystallographically imposed plane of symmetry containing Cu, C, O, B, and one of the pyrazole rings. The structure was solved by Patterson methods followed by successive cycles of full-matrix least-squares refinement and difference Fourier analysis using the Siemens SHELXTL (PC version 5) software package.[29] All the non-hydrogen atoms were refined anisotropically. The hydrogen on B was located from the difference map and refined with a fixed U(H) value. The remaining hydrogens were included in calculated positions ($U(H) = 1.2[U(C)]$).

Cell dimensions and structure refinement data are listed in Table 1. Atomic coordinates for non-hydrogen atoms are given in the Supporting Information. Selected bond lengths and angles are given in Table 2. ORTEP drawings[30] and the atom-numbering schemes of **5**−**7** are shown in Figures 1−3, respectively. Full crystallographic data, complete lists of bond distances and angles, anisotropic thermal parameters, and hydrogen coordinates for **5**−**7** are presented in the Supporting Information.

Table 2. Selected Bond Distances (Å) and Angles (deg)

	$[HB(3,5-(CF_3)_2Pz)_3]Mn(CO)_3$	$[HB(3-(CF_3)Pz)_3]Mn(CO)_3$
Mn−N	2.115(3) 2.120(3) 2.130(3)	2.137(4) 2.119(3) 2.119(3)
Mn−C	1.801(4) 1.804(4) 1.816(4)	1.807(6) 1.812(6) 1.799(5)
C−O	1.143(5) 1.156(5) 1.147(5)	1.145(6) 1.148(6) 1.151(6)
B-N	1.536(5) 1.541(5) 1.540(5)	1.533(6) 1.529(6) 1.537(6)
N−N	1.365(4) 1.362(4) 1.364(4)	1.360(5) 1.360(5) 1.364(5)
Mn···B	3.169	3.171
Mn−C−O	176.2(4) 174.5(4) 174.1(4)	177.5(5) 174.6(6) 176.5(5)

	$[HB(3,5-(CF_3)_2Pz)_3]CuCO$	$[HB(3-(CF_3)Pz)_3]CuCO$
Cu−N	2.035(3) 2.061(2) 2.061(2)	2.039(3) 2.058(2) 2.058(2)
Cu−C	1.808(4)	1.790(4)
C−O	1.110(5)	1.126(5)
B−N	1.565(4) 1.569(3) 1.569(3)	1.558(6) 1.547(3) 1.547(3)
N−N	1.357(4) 1.354(3) 1.354(3)	1.370(4) 1.368(3) 1.368(3)
Cu···B	3.075	3.062
Cu−C−O	179.8(4)	179.0(4)

Calculations. All calculations were done within the PRDDO/M approximations.[31,32] PRDDO/M, an enhanced version

---

(30) Johnson, C. K. ORTEP II; Report ORNL-5138; Oak Ridge National Laboratory: Oak Ridge, TN, 1976.

(31) Derecskei-Kovacs, A.; Marynick, D. S. *Int. J. Quantum Chem.* **1996**, *58*, 193.

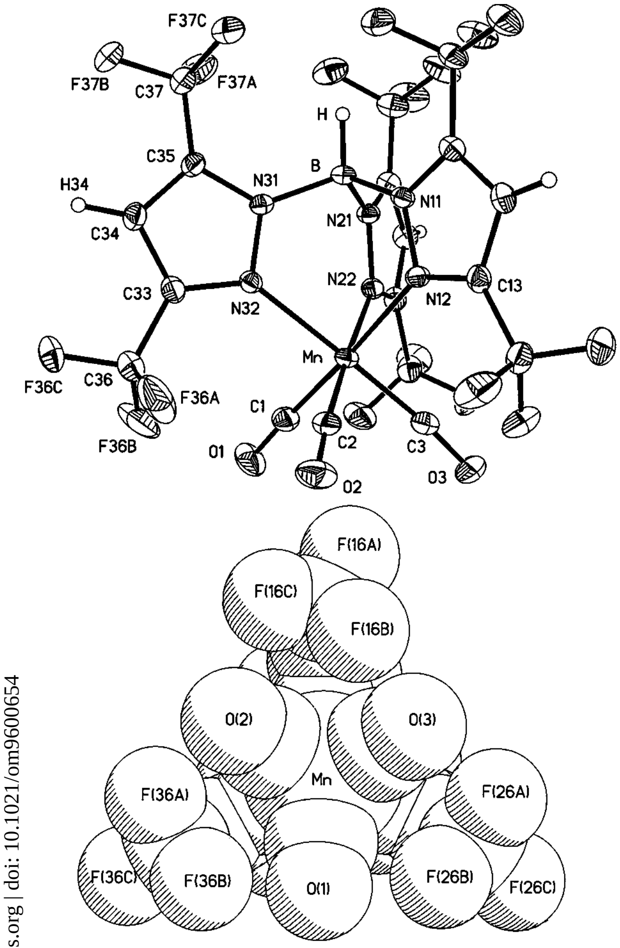

Figure 1. (A, top) Structure and atom-numbering scheme for $[HB(3,5-(CF_3)_2Pz)_3]Mn(CO)_3$ (thermal ellipsoids at 30% level) and (B, bottom) a view down the Mn···B axis (space-filling model).

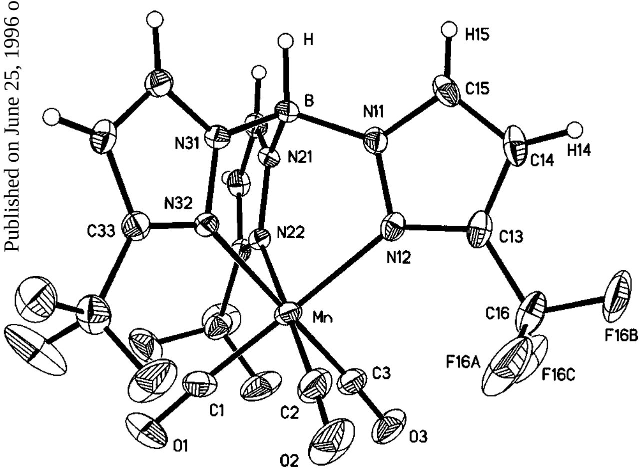

Figure 2. Structure and atom-numbering scheme for $[HB(3-(CF_3)Pz)_3]Mn(CO)_3$ (thermal ellipsoids at 30% level).

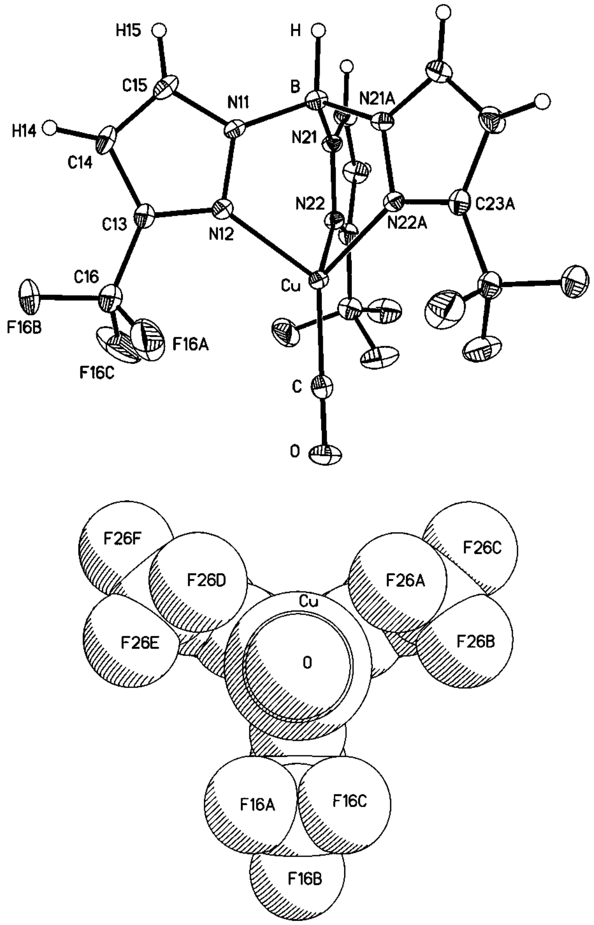

Figure 3. Structure and atom-numbering scheme for $[HB(3,5-(CF_3)_2Pz)_3]CuCO$ (thermal ellipsoids at 30% level) and (B, bottom) a view down O-C bond (space-filling model).

of the original PRDDO method,[33−35] is an approximate ab initio approach which accurately mimics the results of ab initio calculations with much less computational effort. For instance, a PRDDO/M calculation on $(Cp_2Ti)_2(\mu\text{-}C_2S_4)$ with 202 basis functions requires 230 s on an IBM RS6000-370. In contrast, an ab initio STO-3G calculation (using Gaussian 92 with direct SCF) requires 5580 s. PRDDO/M utilizes a minimum basis set of Slater orbitals, except for one important exception: The metal d orbitals are described by a contracted double-ζ set of Slater functions. For the manganese systems, the metal basis set was derived from atomic calculations on the ^5D ($3d^44s^2$) state of Mn^+, while the basis set for the copper systems was derived from the ^3F ($3d^84s^2$) state of Cu^+. The 4s/4p exponents were set to 2.0 in both cases. All geometries were fully optimized using gradient techniques within C_3 or C_{3v} symmetry.

Cyclic Voltammetry. Working electrodes were fashioned out of either glassy-carbon or platinum rods that were sealed into a Kel-F shroud. A geometric area of 3.2 mm^2 was exposed to the electrolyte. Electrode surfaces were polished down to 0.05 μm with alumina powder (Buehler) on a wet microcloth and then washed in acetone and dried under N_2 prior to use. The instrumentation for cyclic voltammetry consisted of a Bioanalytical Systems Model CV27 potentiostat/galvanostat operated in conjunction with a Houston Omnigraphic X-Y recorder. A three-electrode cell geometry was used, and a N_2 blanket was maintained over the solution during the experiments. A Pt spiral served as the counter electrode, and a Ag/AgCl/3 M KCl electrode was employed as reference. The latter was separated from the main cell compartment by a fine glass frit. All potentials in this study are quoted with respect to this reference. Acetonitrile or acetonitrile−CH_2Cl_2 (50/50, v/v) were used as solvents, and the supporting electrolyte was tetra-*n*-butylammonium trifluoromethanesulfonate ((TBA)-OTf). The solvents and the electrolyte were purchased from commercial sources and purified using standard methods prior to use.[26]

---

(32) Derecskei-Kovacs, A.; Woon, D. E.; Marynick, D. S. *Int. J. Quantum Chem.*, in press.

(33) Marynick, D. S.; Lipscomb, W. N. *Proc. Natl. Acad. Sci. U.S.A.* **1982**, *79*, 1341.

(34) Halgren, T. A.; Lipscomb, W. N. *Proc. Natl. Acad. Sci. U.S.A.* **1972**, *69*, 652.

(35) Halgren, T. A.; Lipscomb, W. N. *J. Chem. Phys.* **1973**, *58*, 1569.

The concentration of the metal complex in each case was ~10 mM. The potential was first scanned in the positive direction from the open-circuit potential (identifiable in each voltammogram in Figures 4−6 by the discontinuity or break in the curve). The scan direction was switched at the positive limit (nominally between +1.5 and +1.8 V). The negative-going scan in turn was switched at the cathodic limit variable from ca. −0.5 V (e.g., Figure 4) to −1.7 V (e.g., Figure 6), with the cycle finally terminating at the open-circuit potential. The potential scan rate was 150 mV/s in all the voltammograms presented.

Results and Discussion

Manganese Complexes. Synthesis and Structures. The treatment of [HB(3,5-$(CF_3)_2Pz)_3$]Ag(THF) with an equimolar amount of BrMn$(CO)_5$ in THF afforded [HB(3,5-$(CF_3)_2Pz)_3$]Mn$(CO)_3$ (**5**) as a yellow solid (eq 1). It was characterized by NMR and IR spectroscopy, elemental analysis, and X-ray diffraction. The ^1H NMR spectrum of **5** in C_6D_6 contains a singlet at 6.22 ppm corresponding to the hydrogens on the pyrazole rings. This can be compared with the chemical shift value of 5.79 ppm (in $CDCl_3$) for [HB(3,5-$(CH_3)_2Pz)_3$]Mn$(CO)_3$. The ^{19}F NMR spectrum exhibited a singlet and a doublet at −57.2 and −58.7 ppm, respectively. These chemical shift values are in the expected region for CF_3 groups.[36] We believe that the doublet structure of the signal at δ −58.7, which could be assigned to the trifluoromethyl substituents on the pyrazole 5-position, is a result of spin-spin coupling to the hydrogen on boron.

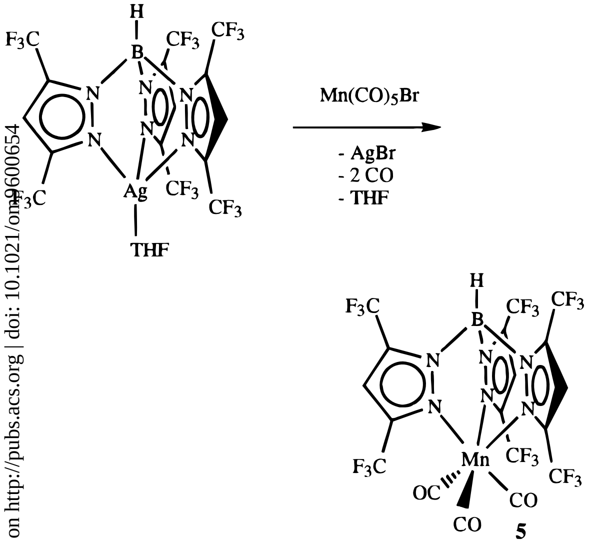

5

(1)

Long-range $^1H-^{19}F$ coupling has been observed in various other metal adducts derived from the [HB(3,5-$(CF_3)_2Pz)_3$]$^-$ ligand system, e.g., [HB(3,5-$(CF_3)_2Pz)_3$]Ag(THF) (^{19}F NMR: δ −58.4 (d), −61.2),[22] [HB(3,5-$(CF_3)_2Pz)_3$]CuCO (^{19}F NMR: δ −58.8 (d), −61.4),[20] or [HB(3,5-$(CF_3)_2Pz)_3$]Na(H_2O) (^{19}F NMR: δ −58.5 (d), −62.2),[19] and has been confirmed by experiments involving the deuterated ligand [DB(3,5-$(CF_3)_2Pz)_3$]$^-$ and from ^1H-decoupled ^{19}F NMR spectroscopy.[19] For example, the resonance corresponding to the CF_3 groups on the pyrazole ring 5-position appears as a singlet in the ^{19}F NMR spectrum of [DB(3,5-$(CF_3)_2Pz)_3$]Na(H_2O) or in the $^{19}F\{^1H\}$ NMR spectrum of [HB(3,5-$(CF_3)_2Pz)_3$]Na(H_2O). We have also synthesized the deuterated analog of **5**, [DB(3,5-$(CF_3)_2Pz)_3$]Mn$(CO)_3$, using [DB(3,5-$(CF_3)_2Pz)_3$]Ag(THF) and BrMn$(CO)_5$. The ^{19}F NMR spectrum of [DB(3,5-$(CF_3)_2Pz)_3$]Mn$(CO)_3$ shows only a singlet for the trifluoromethyl groups on the pyrazole ring 5-position, confirming the involvement of the H on boron in the splitting of the signal centered at −58.7 ppm.

Interestingly, in compound **5**, the ^{19}F NMR resonance due to CF_3 groups on the pyrazole ring 3-position appears at a lower frequency relative to CF_3 groups on the 5-position. We have observed a similar pattern in the low-valent indium species [HB(3,5-$(CF_3)_2Pz)_3$]In (^{19}F NMR: δ −58.4, −58.5 (d)).[22] In contrast, metal adducts such as [HB(3,5-$(CF_3)_2Pz)_3$]CuCO, [HB(3,5-$(CF_3)_2Pz)_3$]Na(H_2O), and [HB(3,5-$(CF_3)_2Pz)_3$]Ag(THF) show an opposite pattern where the ^{19}F NMR signal of the CF_3 groups on the pyrazole ring 3-position appears at a higher frequency relative to CF_3 groups on the 5-position. Overall, the chemical shift value of the fluorines closer to boron in the metal adducts of [HB(3,5-$(CF_3)_2Pz)_3$]$^-$ is relatively constant.[19]

The preparation of [HB(3-$(CF_3)Pz)_3$]Mn$(CO)_3$ (**6**) has been achieved by reacting the corresponding sodium salt, [HB(3-$(CF_3)Pz)_3$]Na(THF) with BrMn$(CO)_5$ (eq 2).

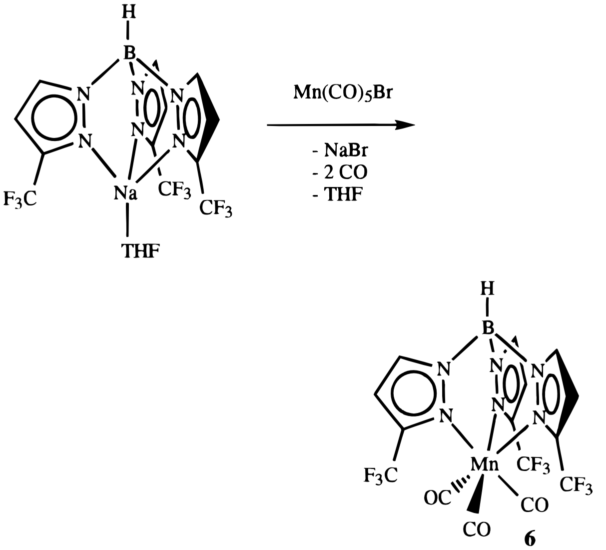

(2)

6

Compound **6** was characterized by ^1H and ^{19}F NMR spectroscopy and IR spectroscopy. The ^{19}F NMR spectrum of **6** shows only a single resonance at −57.4 ppm. This signal appears at a position very close to that observed for the analogous fluorines in compound **5**.

The solid-state infrared spectrum of [HB(3,5-$(CF_3)_2Pz)_3$]Mn$(CO)_3$ (**5**) exhibits two bands at 2065 and 1975 cm^{-1} corresponding to the carbonyl stretching frequencies. The ν_{CO} bands of [HB(3-$(CF_3)Pz)_3$]Mn$(CO)_3$ (**6**) (2054, 1963 cm^{-1}) appeared at a significantly lower frequency compared to those of **5**, suggesting a greater degree of Mn → CO back-bonding (and possibly a reduced σ-bonding) in **6**. This suggests that, in tris(pyrazolyl)borate systems, the substituent on the pyrazole ring 5-position has a significant effect on the electronic properties of the metal ion.

The ν_{CO} values of **5** and **6** can be compared with the corresponding bands in the non-fluorinated analogs (Table 3). For example, the closely related methylated

---

[36] Everett, T. S. In *Chemistry of Organic Fluorine Compounds II*, ACS Monograph 187; Hudlicky, M., Pavlath, A. E., Eds.; American Chemical Society: Washington, DC, 1995; p 1037.

Table 3. Carbonyl Stretching Frequencies (cm^{-1})

compd	ν_{CO}	medium	ref
$[HB(3,5\text{-}(CF_3)_2Pz)_3]Mn(CO)_3$	2065, 1975	KBr	this work
$[HB(3\text{-}(CF_3)Pz)_3]Mn(CO)_3$	2054, 1963	KBr	this work
$[HB(Pz)_3]Mn(CO)_3$	2026, 1915	KBr	37
$[HB(3,5\text{-}(CH_3)_2Pz)_3]Mn(CO)_3$	2023, 1912	KBr	37
$[HB(3,5\text{-}(CF_3)_2Pz)_3]CuCO$	2137	KBr	20
$[HB(3\text{-}(CF_3)Pz)_3]CuCO$	2100	KBr	this work
$[HB(3,5\text{-}(Ph)_2Pz)_3]CuCO$	2086	KBr	40
$[HB(Pz)_3]CuCO$	2083	cyclohexane	41,42
$[HB(3,5\text{-}(CH_3)_2Pz)_3]CuCO$	2066	cyclohexane	42,43
$[HB(3,5\text{-}(i\text{-}Pr)_2Pz)_3]CuCO$	2056	KBr	40
$[\eta^5\text{-}C_5Cl_5]Mn(CO)_3$	2048, 1982	cyclohexane	44
$[\eta^5\text{-}(CF_3)C_5H_4]Mn(CO)_3$	2030, 1942	neat	45
$[\eta^5\text{-}C_5H_5]Mn(CO)_3$	2023, 1935	solid	46
$[\eta^5\text{-}(CH_3)C_5H_4]Mn(CO)_3$	2015, 1915	neat	47
$[\eta^5\text{-}(CH_3)_5C_5]Mn(CO)_3$	2020, 1930	C_6H_6	48
$[\eta^5\text{-}C_5H_5]CuCO$	2093	pentane	49
$[\eta^5\text{-}(CH_3)_5C_5]CuCO$	2075	diethyl ether	50
free CO	2143		51

Table 4. Selected Bond Distances (Å) of Tricarbonyl[tris(pyrazolyl)borato]manganese(I) Complexes

compd	Mn−N	Mn−C	ref
$[HB(Pz)_3]Mn(CO)_3$	2.177(8)	1.81(1)	37
$[PzB(Pz)_3]Mn(CO)_3$	2.064(3) 2.052(3) 2.029(3)	1.802(5) 1.806(4) 1.820(5)	52
$[HB(3,5\text{-}(CH_3)_2Pz)_3]Mn(CO)_3$	2.070(5) 2.069(4) 2.080(4)	1.798(6) 1.782(7) 1.794(6)	37
$[HB(3\text{-}(CF_3)Pz)_3]Mn(CO)_3$	2.137(4) 2.119(3) 2.119(3)	1.807(6) 1.812(6) 1.799(5)	this work
$[HB(3,5\text{-}(CF_3)_2Pz)_3]Mn(CO)_3$	2.115(3) 2.120(3) 2.130(3)	1.801(4) 1.804(4) 1.816(4)	this work

analog $[HB(3,5\text{-}(CH_3)_2Pz)_3]Mn(CO)_3$ shows absorption bands at significantly lower values of 2023 and 1912 cm^{-1}.[37] Lower ν_{CO} values have also been observed for the manganese analog derived from the parent tris(pyrazolyl)borate **1**.[37] These data clearly indicate that, in compounds **5** and **6**, there is a notable reduction in the metal to CO back-bonding. This can be attributed to the presence of powerful electron-withdrawing CF_3 substituents on the tris(pyrazolyl)borate ligand. The manganese coordinated to the weakly donating ligand $[HB(3,5\text{-}(CF_3)_2Pz)_3]^-$ would have a relatively high positive charge. This would lead to a reduction in the Mn → CO back-bonding, thus resulting in a higher C−O stretching frequency. These effects are confirmed by the theoretical calculations (see below). The effect would be lower in **6**, which contains only three CF_3 substituents on the tris(pyrazolyl)borate ligand. Interestingly, the trend observed with the values of ν_{CO} (Table 3) for tris(pyrazolyl)borates is consistent with the electron donating/withdrawing ability of the substituents[38] or with the acid−base properties of the free pyrazoles.[39]

It is noteworthy that in contrast to the previously reported $[HB(3,5\text{-}(CF_3)_2Pz)_3]CuCO$ (ν_{CO} 2137 cm^{-1}) or $[HB(3,5\text{-}(CF_3)_2Pz)_3]AgCO$ (ν_{CO} 2178 cm^{-1}) the ν_{CO} values for compound **5** are significantly lower than that of the free CO molecule (2143 cm^{-1}).[20,21,51] According to the classical metal−CO bonding theories, lower C−O stretching frequencies would be expected when CO is coordinated to metal ions capable of π-donation to a CO moiety. Therefore, the IR data for **5** suggest that (despite the presence of highly electron-withdrawing ligand systems) there is a significant amount of back-bonding between Mn and CO. The metal-CO interaction in $[HB(3,5\text{-}(CF_3)_2Pz)_3]AgCO$ is believed be predominantly σ-type (M ← CO) with very little or no M → CO π-back-bonding.[17,21]

Compounds **5** and **6** were characterized by X-ray crystallography. Figures 1 and 2 show the ORTEP plots of **5** and **6**, respectively. The view of **5** down the Mn···B axis shows a fairly symmetric (close to C_{3v}) molecule. A very similar picture was observed for **6**. The manganese atom in both systems adopts a pseudooctahedral geometry. From the data summarized in Table 2 it is seen that there are no significant differences in the key structural parameters between **5** and **6**.

The Mn−N bond distances of **5** (or **6**) are slightly longer than those observed for the methylated analog $[HB(3,5\text{-}(CH_3)_2Pz)_3]Mn(CO)_3$ (see Table 4).[37] The difference between the Mn−N bond lengths of fluoromethylated and methylated species is presumably a reflection of the reduced donor ability of the electron-deficient fluorinated tris(pyrazolyl)borate ligand. The values observed for $[HB(Pz)_3]Mn(CO)_3$ do not follow the expected trend.[37] However, $[PzB(Pz)_3]Mn(CO)_3$, which has much better experimental uncertainties in its bond distances, agrees fairly well with expectations.

Interestingly, despite large differences in ν_{CO}, the structural parameters of the $Mn(CO)_3$ fragment in **5** or **6** do not differ significantly from those of the nonfluorinated analogs (Table 4). In fact, Mn−C bond lengths of **5** and **6** are nearly identical with the corresponding values in $[HB(3,5\text{-}(CH_3)_2Pz)_3]Mn(CO)_3$ or to those of various other manganese(I) carbonyls (average 1.808 Å for 789 examples).[53]

Tris(pyrazolyl)borate ligands are often considered as cyclopentadienyl analogs in that both classes are monoanionic, six-electron donors capable of occupying three coordination sites around a metal center.[1] Therefore, it is interesting to compare the manganese tricarbonyl derivatives of cyclopentadienyls with those of tris(pyrazolyl)borates. Some of the known manganese

---

(37) Joachim, J. E.; Apostolidis, C.; Kanellakopoulos, B.; Maier, R.; Marques, N.; Meyer, D.; Müller, J.; Pires de Matos, A.; Nuber, B.; Rebizant, J.; Ziegler, M. L. *J. Organomet. Chem.* **1993**, *448*, 119.

(38) Gordon, A. J.; Ford, R. A. *The Chemist's Companion*; Wiley: New York, 1972; p 145.

(39) Elguero, J.; Yranzo, G. I.; Laynez, J.; Jimenez, P.; Menendez, M.; Catalan, J.; de Paz, J. L. G.; Anvia, F.; Taft, R. W. *J. Org. Chem.* **1991**, *56*, 3942.

(40) Kitajima, N.; Fujisawa, K.; Fujimoto, C.; Moro-oka, Y.; Hashimoto, S.; Kitagawa, T.; Toriumi, K.; Tatsumi, K.; Nakamura, A. *J. Am. Chem. Soc.* **1992**, *114*, 1277.

(41) Bruce, M. I.; Ostazewski, A. P. P. *J. Chem. Soc., Dalton Trans.* **1973**, 2433.

(42) Bruce, M. I. *J. Organomet. Chem.* **1972**, *44*, 209.

(43) Mealli, C.; Arcus, C. S.; Wilkinson, J. L.; Marks, T. J.; Ibers, J. A. *J. Am. Chem. Soc.* **1976**, *98*, 711.

(44) Reimer, K. J.; Shaver, A. *Inorg. Chem.* **1975**, *14*, 2707.

(45) Gassman, P. G.; Winter, C. H. *J. Am. Chem. Soc.* **1986**, *108*, 4228.

(46) Cotton, F. A.; Liehr, A. D.; Wilkinson, G. *J. Inorg. Nucl. Chem.* **1955**, *1*, 175.

(47) Parker, D. J. *Spectrochim. Acta* **1975**, *31A*, 1789.

(48) Arsenault, C.; Bougeard, P.; Sayer, B. G.; Yeroushalmi, S.; McGlinchey, M. J. *J. Organomet. Chem.* **1984**, *265*, 283.

(49) Cotton, F. A.; Marks, T. J. *J. Am. Chem. Soc.* **1970**, *92*, 5114.

(50) Macomber, D. W.; Rausch, M. D. *J. Am. Chem. Soc.* **1983**, *105*, 5325.

(51) Braterman, P. S. *Metal Carbonyl Spectra*; Academic Press: New York, 1975; p 177.

(52) MacNeil, J. H.; Roszak, A. W.; Baird, M. C.; Preston, K. F.; Rheingold, A. L. *Organometallics* **1993**, *12*, 4402.

(53) Orpen, A. G.; Brammer, L.; Allen, F. H.; Kennard, O.; Watson, D.; Taylor, R. *J. Chem. Soc., Dalton Trans.* **1989**, S1.

carbonyl complexes and their C−O stretching frequencies are listed in Table 3.[54] The carbonyl stretching frequency values of **5** are significantly higher than those observed for [η^5-(CF_3)C_5H_4]Mn(CO)$_3$.[45] However, they are much closer to that of [η^5-C_5Cl_5]Mn(CO)$_3$ (average 2015 *vs* 2020 cm^{-1} for **5**).[44] This is interesting when considering the fact that the group electronegativity of CF_3 is only slightly higher than that of Cl.[55] Unfortunately, [η^5-(CF_3)$_5C_5$]Mn(CO)$_3$, which would have been a better comparison for **5**, is still unknown. This may partly be a result of the difficulties associated with the synthesis of its precursor ligand.[56,57] Nevertheless, on the basis of the currently available data, [HB(3,5-(R)$_2$Pz)$_3$]Mn(CO)$_3$ systems in general seem to have slightly lower C−O stretching frequencies compared to those of [η^5-(R)$_5C_5$]Mn(CO)$_3$.

Theoretical Study. In order to understand the effects of CF_3 groups on the structure and bonding of manganese tris(pyrazolyl)borates, we have carried out a PRDDO/M calculation. This method, which is an approximate ab initio approach, has been shown to yield reasonable geometries in a wide variety of transition-metal complexes[58,59] and has proven useful in many problems involving structure and conformation in inorganic and organometallic systems.[60−69] In Table 5, we compare the calculated and experimental values for the important geometrical parameters of [PzB(Pz)$_3$]Mn(CO)$_3$, [HB(3-(CF_3)Pz)$_3$]Mn(CO)$_3$, and [HB(3,5-(CF_3)$_2$Pz)$_3$]Mn(CO)$_3$. To compare our calculated geometries to experimental ones, in the manganese systems we chose [PzB(Pz)$_3$]$^-$ (rather than [HB(Pz)$_3$]$^-$) as the parent system ligand. This choice was made because the [PzB(Pz)$_3$]Mn(CO)$_3$ crystal structural data appear to be somewhat more reliable. In addition, we have fully optimized the structures of [HB(Pz)$_3$]Mn(CO)$_3$ and [PzB(Pz)$_3$]Mn(CO)$_3$ and find only minor differences in the metal−ligand bond lengths (the difference is 0.012 Å for the M−N distance, while the calculated Mn−C distances are exactly the same).

In general, the agreement between calculated and experimental distances is excellent. Trifluoromethyl substituents on the tris(pyrazoyl)borate ligand decrease the σ-donating ability of the coordinating nitrogens and lengthen the Mn−N bond. The effect of fluoro substitution can be clearly seen in calculations on the free ligands. The coordinating nitrogen "lone-pair" orbitals are on average 1.61 eV lower in energy in **3** as compared to **1**. The effect on the Mn−N bond length is dramatic: As one proceeds from the parent ligand to the partially fluorinated ligand **4**, the Mn−N bond lengthens by 0.077 Å (with a corresponding PRDDO/M-calculated value of 0.074 Å). However, complete fluoro substitution (ligand **3** *vs* **4**) has essentially no effect on the geometry around the metal.

Table 5. Experimental and Calculated Structural Parameters

[PzB(Pz)$_3$]Mn(CO)$_3$

	exptl[a]	calcd
Mn−N	2.048 (0.013)	2.076
Mn−C	1.809 (0.007)	1.779
C−O	1.137 (0.003)	1.147

[HB(3-(CF_3)Pz)$_3$]Mn(CO)$_3$

	exptl[b]	calcd
Mn−N	2.125 (0.008)	2.150
Mn−C	1.806 (0.005)	1.815
C−O	1.148 (0.002)	1.145

[HB(3,5-(CF_3)$_2$Pz)$_3$]Mn(CO)$_3$

	exptl[b]	calcd
Mn−N	2.122 (0.006)	2.151
Mn−C	1.807 (0.006)	1.819
C−O	1.149 (0.005)	1.144

[a] Reference 52. All distances are in Å. The experimental numbers are the averages (standard deviations) of the three distances assumed to be symmetry equivalent in the calculated geometries. [b] This work.

Due to experimental uncertainty, the crystallographic trends in the Mn−C distances are difficult to discern; however, the PRDDO/M trend is clear. Increasing fluoro substitution should result in a more positively charged metal, which back-bonds less to the carbonyls and results in a lengthening of the Mn−C distance and a shortening of the C−O distance. Indeed, the group charge of the N_3Mn(CO)$_3$ moiety is −0.17e for the parent complex and −0.07e for the fully fluorinated complex. This leads to a reduction of carbonyl back-bonding, which is clearly seen in the d orbital populations (5.312e for [HB(Pz)$_3$]Mn(CO)$_3$ and 5.362e for [HB(3,5-(CF_3)$_2$Pz)$_3$]Mn(CO)$_3$). The Mulliken population analysis suggests that there is essentially no Mn−Pz π-bonding. If we examine the nitrogen in one of the approximate mirror planes of the molecule (the fluorinated species have C_3 symmetry but the tris(pyrazolyl)borate frame work is basically C_{3v}), we can cleanly separate σ- and π-effects for the Mn−N bonding interaction. For [HB(Pz)$_3$]Mn(CO)$_3$ the Mn−N overlap population is 0.192, of which 0.178 is due to σ-type orbital interactions. The corresponding overlap populations for the fully fluorinated systems are 0.176 and 0.165. It is therefore clear that the metal−nitrogen π−bonding effects are minimal in these systems.

Copper Complexes. Synthesis and Structure. [HB(3-(CF_3)Pz)$_3$]CuCO (**7**) was prepared from CuOTf, CO and [HB(3-(CF_3)Pz)$_3$]Na(THF) and isolated as a colorless, air-stable solid (eq 3). It was characterized by NMR and IR spectroscopy, elemental analysis, and X-ray crystallography. The infrared spectrum of **7** has a sharp band at 2100 cm^{-1}, assigned to C−O stretching. This value is much lower than that observed for [HB(3,5-(CF_3)$_2$Pz)$_3$]CuCO (2137 cm^{-1}).[20] The C−O stretch-

---

[54] IR data for these compounds in the same medium are currently not available. This (due to possible medium effects on ν_{CO}) hinders a more rigorous data analysis.

[55] Huheey, J. E.; Keiter, E. A.; Keiter, R. L. *Inorganic Chemistry*, 4th ed.; Harper Collins: New York, 1993; pp 182−197.

[56] Laganis, E. D.; Lemal, D. M. *J. Am. Chem. Soc.* **1980**, *102*, 6633.

[57] Chambers, R. D.; Mullins, S. J.; Roche, A. J.; Vaughan, J. F. S. *J. Chem. Soc., Chem. Commun.* **1995**, 841.

[58] Marynick, D. S.; Axe, F. U.; Kirkpatrick, C. M.; Throckmorton, L. *Chem. Phys. Lett.* **1983**, *99*, 406.

[59] Marynick, D. S.; Reid, R. D. *Chem. Phys. Lett.* **1986**, *124*, 17.

[60] Marynick, D. S.; Axe, F. U. *J. Am. Chem. Soc.* **1988**, *110*, 3728.

[61] Hansen, L. M.; Marynick, D. S. *J. Am. Chem. Soc.* **1988**, *110*, 2358.

[62] Jolly, C. A.; Marynick, D. S. *J. Am. Chem. Soc.* **1989**, *111*, 7968.

[63] Hansen, L. M.; Marynick, D. S. *Organometallics* **1989**, *8*, 2173.

[64] Hansen, L. M.; Marynick, D. S. *Inorg. Chem.* **1990**, *29*, 2482.

[65] Lawless, M.; Marynick, D. S. *Inorg. Chem.* **1991**, *30*, 3547.

[66] Lawless, M.; Marynick, D. S. *J. Am. Chem. Soc.* **1991**, *113*, 7513.

[67] Kumar, P. N. V. P.; Marynick, D. S. *Inorg. Chem.* **1993**, *32*, 1857.

[68] Rogers, J. R.; Wagner, T. P. S.; Marynick, D. S. *Inorg. Chem.* **1994**, *33*, 3104.

[69] Rogers, J. R.; Johnson, C. K.; Marynick, D. S. *Inorg. Chem.* **1994**, *33*, 4566.

[70] Churchill, M. R.; DeBoer, B. G.; Rotella, F. J.; Abu Salah, O. M.; Bruce, M. I. *Inorg. Chem.* **1975**, *14*, 2051.

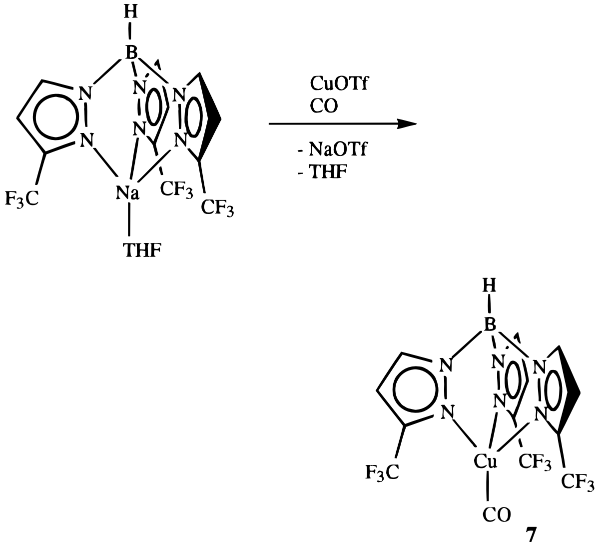

(3)

7

ing frequencies of a series of [tris(pyrazolyl)borato]-copper carbonyls are listed in Table 3. As with the manganese adducts, the order observed with the C−O stretching frequencies relates closely to the electron donor ability of the tris(pyrazolyl)borate ligand.

The X-ray crystal structure of **7** is illustrated in Figure 3. The copper atom adopts a pseudo-tetrahedral geometry. The Cu−C−O moiety is linear within experimental limits. The Cu−C and C−O bond lengths are 1.790(4) and 1.126(5) Å, respectively. These values can be compared to the corresponding distances in $[HB(3,5-(CF_3)_2Pz)_3]CuCO$ (Cu−C = 1.808(4), C−O = 1.110(5) Å)[20] or $[HB(3,5-(i\text{-}Pr)_2Pz)_3]CuCO$ (Cu−C = 1.769(8), C−O = 1.118(10) Å).[40] The Cu−C bond lengths are in agreement with the expected trend based on the C−O stretching frequency.

The relative effects of having trifluoromethyl groups on the pyrazole ring 5-position are more noticeable (particularly from the C−O stretching frequency) in the copper derivatives. For example, the difference in ν_{CO} between $[HB(3,5-(CF_3)_2Pz)_3]CuCO$ and $[HB(3-(CF_3)Pz)_3]CuCO$ is about 37 cm^{-1}, whereas in the manganese systems $[HB(3,5-(CF_3)_2Pz)_3]Mn(CO)_3$ and $[HB(3-(CF_3)Pz)_3]Mn(CO)_3$ it is about 12 cm^{-1}. This may be due to the fact that, in copper systems, the ligand effects are concentrated only on one CO group, whereas in Mn complexes these effects are shared over three equivalent CO groups. However, the lowering of ν_{CO} relative to that of free CO is more pronounced in the manganese complexes. For example, $[HB(3,5-(CF_3)_2Pz)_3]CuCO$ has a ν_{CO} value only slightly lower than that in CO (2143 cm^{-1}). In contrast, $[HB(3,5-(CF_3)_2Pz)_3]Mn(CO)_3$ displays a significantly lower C−O stretching frequency (average reduction of 123 cm^{-1}). The difference between the ν_{CO} values of CO and $[HB(3-(CF_3)Pz)_3]CuCO$ or $[HB(3-(CF_3)Pz)_3]Mn(CO)_3$ is about 43 and 134 cm^{-1}, respectively. These values reflect the relative effectiveness of metal → CO back-bonding, which is notably higher for manganese than for copper.

It is also possible to compare the copper(I) carbonyl complexes of tris(pyrazolyl)borates with those of cyclopentadienyl ligands.[54] In contrast to manganese, copper carbonyls derived from cyclopentadienyls are rare and significantly less stable.[49,50] Nevertheless, the data listed in Table 3 show that, as with manganese, ν_{CO} of $[HB(3,5-(R)_2Pz)_3]CuCO$ appears at a slightly lower value compared to that of $[\eta^5-(R)_5C_5]CuCO$.

Table 6. Experimental and Calculated Structural Parameters

$[HB(Pz)_3]CuCO$

	exptl[a]	calcd
Cu−N	2.051 (0.009)	2.041
Cu−C	1.755	1.759
C−O	1.120	1.155

$[HB(3-(CF_3)Pz)_3]CuCO$

	exptl[b]	calcd
Cu−N	2.052 (0.009)	2.061
Cu−C	1.790	1.769
C−O	1.126	1.152

$[HB(3,5-(CF_3)_2Pz)_3]CuCO$

	exptl[c]	calcd
Cu−N	2.052 (0.012)	2.058
Cu−C	1.808	1.771
C−O	1.110	1.151

[a] Reference 70. All distances are in Å. The experimental numbers are the averages and standard deviations from two independent molecules. [b] This work. [c] Reference 20.

Theoretical Calculations. A comparison of calculated and experimental distances for $[HB(Pz)_3]CuCO$, $[HB(3-(CF_3)Pz)_3]CuCO$, and $[HB(3,5-(CF_3)_2Pz)_3]CuCO$ is presented in Table 6. While exact comparisons are again difficult because of experimental uncertainties, some of the same trends are evident. Increasing the degree of fluorination lengthens the Cu−C bond and shortens the C−O bond. The effect on the Cu−N bond length is less clear, although structural data on alkyl-substituted systems do suggest that the Cu−N bond lengthens upon fluorination. For instance the 3,5-diisopropyl derivative[40] has a Cu−N bond length of 2.018 Å, compared to 2.052 Å for the fluorinated species. The theoretical calculations exhibit very similar trends. The reduced back-bonding in the fluorinated system is also evident in the copper complexes. For example, the sums of the d-orbital populations for the parent and fluorinated copper complexes are 9.37e and 9.42e, respectively (these are formally d^{10} complexes). It should be noted that there is very little d-orbital participation in the Cu−ligand σ bonds. To demonstrate this fact, we performed a Boys localization on the PRDDO wave functions and calculated the sum of the d-orbital populations in all four Cu−ligand σ bonds. We found a d-orbital contribution of 0.027e for the parent system and 0.025e for the fluorinated system. Therefore, the d-orbital population differences observed between the parent and fluorinated species are due to back-bonding.

Cyclic Voltammetry. In order to further explore the electronic effects associated with substitution on the tris(pyrazolyl)borate ligand, cyclic voltammetry was performed on methylated and trifluoromethylated tris(pyrazolyl)borate derivatives of copper(I). Copper (rather than manganese) was selected as the metal center in the complexes for these experiments in view of the fact that Cu(0) ↔ Cu(I) ↔ Cu(II) electrochemistry[71] affords a well-behaved probe for studying the electronic effects. The secondary ligand on the copper center was also

---

(71) Napp, D. T.; Johnson, D. C.; Bruckenstein, S. *Anal. Chem.* **1967**, *39*, 481.

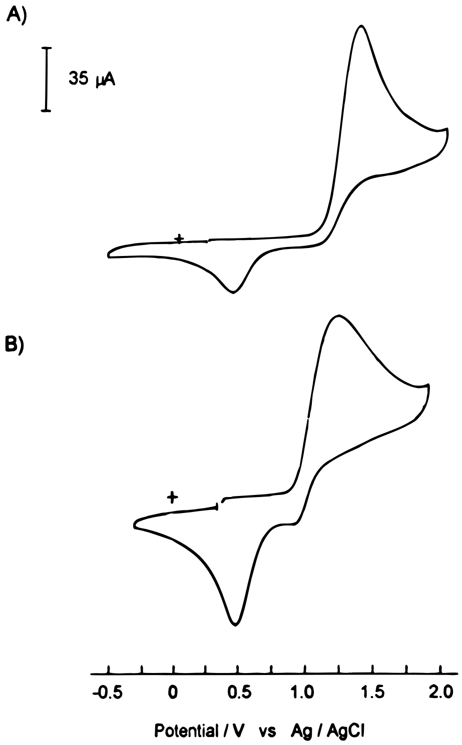

Figure 4. Cyclic voltammograms for (A) [HB(3,5-$(CF_3)_2$-$Pz)_3$]$CuPPh_3$ and (B) [HB(3,5-$(CF_3)_2Pz)_3$]$CuNCCH_3$ at glassy carbon in CH_3CN + 0.1 M (TBA)OTf. Scan conditions are noted in the Experimental Section.

varied in these experiments as an additional probe of its influence on the redox characteristics of the resultant complex.

That fluorination of the tris(pyrazolyl)borate ligand exerts a direct effect on the ease of oxidation of the corresponding complex is seen by a comparison of the cyclic voltammograms for the fluoro (Figure 4A) and non-fluoro (Figure 5A) copper complexes. The anodic wave corresponding to the Cu(I) → Cu(II) process is shifted by ~500 mV (from ca. 1.0 to ca. 1.5 V) in the positive direction as a result of fluoro substitution. The oxidations of all the copper compounds examined in this study were irreversible and featured coupled chemical reactions pursuant to electrochemical generation of the Cu(II) state. Nonetheless, it is interesting that the cathodic reduction waves on the return cycle manifest themselves at almost identical locations for the two complexes bearing disparate axial ligands, CH_3CN and PPh_3, respectively (compare parts A and B of Figures 4). This suggests that ligand substitution (from the electrolyte) occurs in the latter case concomitant with copper oxidation such that, in both cases, it is the Cu^{II}–CH_3CN complex that is being reduced. There is precedence for ligand dissociation and reactions involving the electrolyte species in previous voltammetry data on 3-*tert*-butyl- and 3,5-diphenyl-substituted tris(pyrazolyl)borate complexes of Cu(I).[72]

The Cu(I) → Cu(0) redox process can be observed when the voltammograms are scanned to negative potentials, as exemplified by the scans in Figure 6. The sharp anodic waves on the return (positive-going) cycle in Figure 6A,B correspond to the stripping of copper from the Pt and glassy-carbon surfaces, respectively.[73]

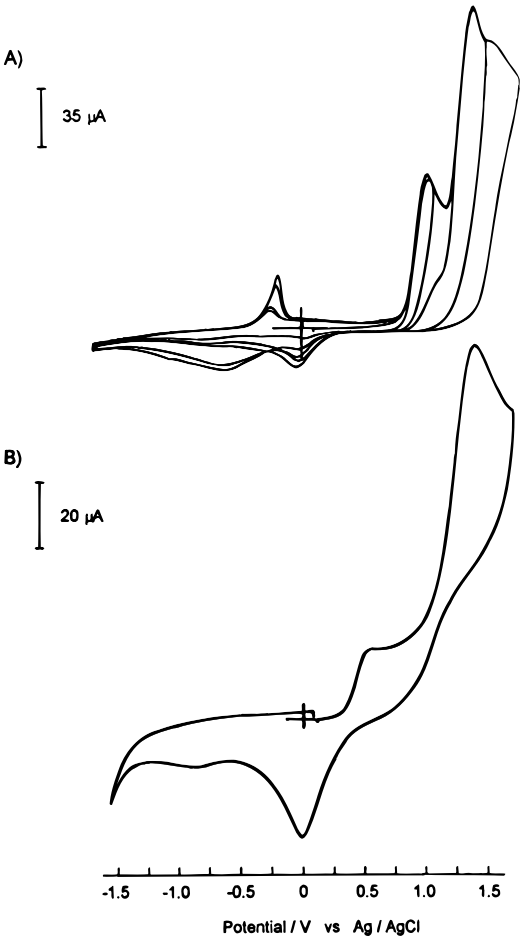

Figure 5. Cyclic voltammograms for (A) [HB(3,5-$(CH_3)_2$-$Pz)_3$]$CuPPh_3$ and (B) [HB(3,5-$(CH_3)_2Pz)_3$]CuCO at Pt in CH_3CN + 0.1 M (TBA)OTf.

Interestingly, the copper deposition process is very sensitive to the nature of the electrode surface, being catalyzed by Pt (Figure 6A), and is relatively sluggish at the glassy-carbon surface (Figure 6B). Copper deposition may occur through a reaction process similar to that shown in eq 4. In fact, as described in a previous

$$[HB(3,5\text{-}(CF_3)_2Pz)_3]CuL + e^- \rightarrow [HB(3,5\text{-}(CF_3)_2Pz)_3]CuL^- \rightarrow [HB(3,5\text{-}(CF_3)_2Pz)_3]^- + Cu + L \quad (4)$$

publication,[19] our attempts to synthesize [HB(3,5-$(CF_3)_2$-$Pz)_3$]$CuCN^-$ led to the removal of copper ion from the [tris(pyrazolyl)borato]copper complex leaving the "naked" [HB(3,5-$(CF_3)_2Pz)_3$]$^-$ ion, which was isolated and characterized as its Et_4N^+ salt.

The electronic effects of ligand substitution also manifest themselves in the reduction behavior. Thus, the non-fluoro compound in Figure 5A shows a sluggish tendency toward reduction relative to its fluoro counterpart (Figure 4A). This is readily seen by a direct comparison of the amplitude of the Cu(0) stripping waves in the two cases. Interestingly, Cu(I) reduction to Cu(0) is completely suppressed when the secondary ligand is CO (Figure 5B), attesting to the stabilization of the Cu(I) oxidation state by the CO ligand.

---

[72] Carrier, S. M.; Ruggiero, C. E.; Houser, R. P.; Tolman, W. B. *Inorg. Chem.* **1993**, *32*, 4889.

[73] Basak, S.; Zacharias, P. S.; Rajeshwar, K. *J. Electroanal. Chem. Interfacial Electrochem.* **1991**, *319*, 111.

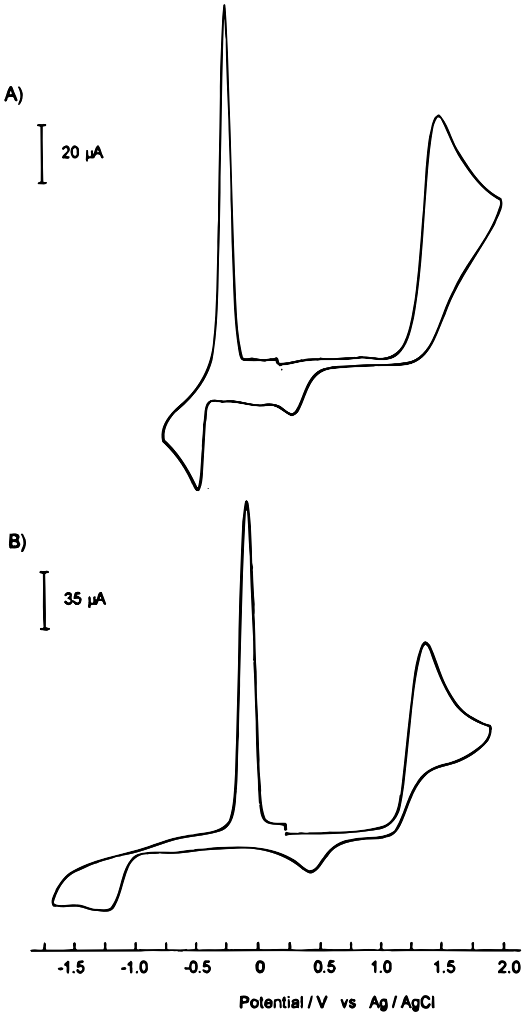

Figure 6. Cyclic voltammograms for $[HB(3,5\text{-}(CF_3)_2Pz)_3]CuPPh_3$ at (A) Pt and (B) glassy carbon in $CH_3CN + 0.1$ M (TBA)OTf.

Finally, it is instructive to compare the oxidation potentials (E_{pa}) of the fluoro derivatives of Cu(I) in this study with previously reported values for other [tris(pyrazolyl)borato]metal complexes. A series of Cu(I) complexes containing 3-*tert*-butyl and 3,5-diphenyl substituents on the tris(pyrazolyl)borate ligand had oxidation potentials varying from ca. 0.70 to ca. 1.0 V.[72] The effect of increasing the metal−nitrogen distances on the electronic properties of the iron center was probed by phenyl substitution on the 3-position of the pyrazole ring.[74] The redox potential for the Fe(III)/Fe(II) couple was observed to shift from 0.23 V for the parent $[HB(Pz)_3]_2Fe$ complex to ∼0.90 V for the sterically encumbered counterpart.[74,75] On the other hand, the Mn complex $[HB(3\text{-}(Ph)Pz)_3]_2Mn$, showed only irreversible waves at potentials approaching the solvent limit, whereas $[HB(3,5\text{-}(Me)_2Pz)_3]_2Mn$ exhibited a Mn(III)/Mn(II) reduction potential at ca. 0.02 V.[74] It is worthy of note that the E_{pa} values observed in this study for the Cu(I) fluoro derivatives are among the highest observed for metal tris(pyrazolyl)borate complexes in general. Correspondingly, the fluoro complexes are also amenable to reduction, thanks to the stabilizing properties of the trifluoromethyl group (relative to its methyl counterpart).

Summary and Conclusions

We have reported the synthesis of manganese and copper complexes derived from highly fluorinated tris(pyrazolyl)borate ligands. The manganese adducts **5** and **6** show significantly high C−O stretching frequencies, suggesting the presence of relatively electron poor metal centers. The copper carbonyl adduct **7** also exhibits a relatively high carbonyl stretching frequency. The order of ν_{CO} values of manganese and copper carbonyls is consistent with that expected from the electron-donating property of the tris(pyrazolyl)borate ligand. In general, manganese complexes show notable reductions in ν_{CO} compared to that of free CO. The effects of the 5-CF_3 substitution on ν_{CO} is more pronounced in copper adducts. Overall, IR spectroscopy results of Mn and Cu carbonyls show CF_3 substituents at the pyrazole ring 5-position to exert a significant effect on the electronic properties of the metal center. Cyclic voltammetry data for the copper complexes show high oxidation potential values for the fluorinated analogs.

The structural parameters resulting from the theoretical studies on these systems are in excellent agreement with the experimental values. Calculations show that with an increasing degree of fluorination the metal−C bond elongates and the C−O distance shortens. This is consistent with the results from the IR study. The Mn−N distances show a large variation, whereas Cu−N lengths seem to be relatively insensitive to the fluorine substitution. The results from the PRDDO/M data also suggest that the bonding between the metal center and the tris(pyrazolyl)borate is almost exclusively a σ-interaction. The calculated rotation barrier of the CF_3 groups of $[HB(3,5\text{-}(CF_3)_2Pz)_3]CuCO$ are 0.54 kcal/mol on the metal side and 4.5 kcal/mol on the B−H side. This and the comparisons to alkyl-substituted tris(pyrazolyl)borate derivatives suggest that the differences in the structural and spectroscopic parameters of fluorinated and non-fluorinated systems are primarily a result of ligand electronic effects.

The ν_{CO} values of manganese and copper carbonyl derivatives of tris(pyrazolyl)borates show close similarities to cyclopentadienyl complexes. In general, C−O stretching frequencies of $[HB(3,5\text{-}(R)_2Pz)_3]Mn(CO)_3$ or $[HB(3,5\text{-}(R)_2Pz)_3]CuCO$ are only slightly lower compared to those of $[\eta^5\text{-}(R)_5C_5]Mn(CO)_3$ or $[\eta^5\text{-}(R)_5C_5]CuCO$. It would be interesting to see whether this will be true for $[\eta^5\text{-}(CF_3)_5C_5]^-$ derivatives of copper and manganese.

Acknowledgment. Financial support received from The Robert A. Welch Foundation (Grants Y-1289 (H.V.R.D.) and Y-743 (D.S.M.)) is gratefully acknowledged. We also thank UTA for providing funds to purchase the Siemens P4 single-crystal X-ray diffractometer.

Supporting Information Available: Tables of crystallographic data, atomic coordinates, thermal parameters, and complete bond distances and angles for **5**−**7** (16 pages). Ordering information is given on any current masthead page.

OM9600654

---

(74) Eichhorn, D. M.; Armstrong, W. H. *Inorg. Chem.* **1990**, *29*, 3607.

(75) Oliver, J. D.; Mullica, D. F.; Hutchinson, B. B.; Milligan, W. O. *Inorg. Chem.* **1980**, *19*, 165.